Biomed Microdevices (2006) 8:277–290
DOI 10.1007/s10544-006-0031-2

Multiscale modeling of protein transport in silicon membrane nanochannels. Part 1. Derivation of molecular parameters from computer simulations

Sabrina Pricl · Marco Ferrone · Maurizio Fermeglia · Francesco Amato · Carlo Cosentino · Mark Ming-Cheng Cheng · Robert Walczak · Mauro Ferrari

Published online: 25 September 2006

Abstract We report in this account our efforts in the development of a novel multiscale simulation tool for integrated nanosystem design, analysis and optimization based on a three-tiered modeling approach consisting of (i) molecular models, (ii) atomistic molecular dynamics simulations, and (iii) dynamical models of protein transport at the continuum scale. In this work we used molecular simulations for the analysis of lysozyme adsorption on a pure silicon surface. The molecular modeling procedures adopted allowed (a) to elucidate the specific mechanisms of interaction between the biopolymer and the silicon surface, and (b) to derive molecular energetic and structural parameters to be employed in the formulation of a mathematical model of diffusion through silicon-based nanochannel membranes, thus filling the existing gap between the nano—and the macroscale.

Keywords Multiscale modeling · Protein transport · Non-Fickian release · Nanochannel membranes

S. Pricl (✉) · M. Ferrone · M. Fermeglia
Molecular Simulation Engineering (MOSE) Laboratory, Department of Chemical Engineering, University of Trieste, Piazzale Europa 1, 34127 Trieste, Italy
e-mail: sabrina.pricl@dicamp.units.it

F. Amato · C. Cosentino
Department of Experimental and Clinical Medicine, Università degli Studi Magna Graecia, via T. Campanella 115, 88100 Catanzaro, Italy

M. M.-C. Cheng · R. Walczak
Division of Hematology and Oncology, Department of Internal Medicine, Ohio State University, 1654 Upham Drive, Columbus, Ohio 43210, USA

M. Ferrari
The University of Texas Health Science Center at Houston, 7000 Fannin, Houston, TX 77030, USA

M. Ferrari
The University of Texas M. D. Anderson Cancer Center, 1515 Holcombe Blvd, Houston, TX 77030, USA

M. Ferrari
Rice University, 6100 Main, Houston, TX 77005, USA

1 Introduction

Nanotechnology, as generally accepted, is concerned with the structures, properties, and processes involving materials having organizational features on the spatial scale of 1–300 nm. At this scale, devices may lead to dramatically enhanced performance, sensitivity, and reliability with considerably decreased size, weight, and cost. Indeed, these scales can lead to new phenomena, providing opportunities for new levels of sensing, manipulation, and control. However, being much smaller than the wavelength of visible light, but much larger than simple molecules, it is difficult to characterize the structure and to control the processes involving nanomaterials. And because it is difficult to see what we are doing at the nanoscale, it is essential to develop theoretical and computational approaches sufficiently fast and accurate that the structure and property of the materials can be predicted for various conditions as a function of time. A particular advantage of using theory is that the properties of new materials can be predicted in advance of experiments. This allows the system to be adjusted and refined (or designed) so as to obtain the optimal properties before the arduous experimental task of synthesis and characterization. However, there are significant challenges in using theory to predict accurate properties for nanoscale materials, especially when biomacromolecules are involved. Indeed, despite the tremendous advances made in the modeling of the structural, thermal, mechanical and

transport properties of materials at the macroscopic level (i.e., finite element analysis of complex structures or continuum simulations), there remains a remarkable uncertainty about how to predict many critical properties related to final performance. The main problem lies in the fact that most of these properties depend on the interactions and chemistry taking place at the atomic level, involving electronic and atomic descriptions at the level of nanometers in the length scale, and picoseconds in the timescale. Conversely, the material designer needs answers from macroscopic modeling (the "finite element paradigm") of components having scales of the order of centimeters, and of phenomena taking place in a time range of milliseconds or much larger. Thus, to achieve a dramatic advancement in the skill of designing innovative, highly-performing materials, it is mandatory that we link the chemistry (micro) to the macroscopic (finite elements or continuum) modeling.

The actual computational modeling of biological macromolecules, mainly based on molecular dynamics (MD) simulations, commonly revolves around structure representations in atomic or near-atomic detail, with a classical description of physical interactions. Such models have been quite successful in complementing experimental data with structural, dynamic, and energetic information, but involve substantial computational resources for larger systems, or when long time scales have to be considered. In particular, structure-activity calculation applications, the formation and interaction of supramolecular assemblies, and the prediction of kinetic and transport phenomena become prohibitive, if feasible at all, with models at atomic details. Thus, we need to develop some computational strategy to link the atomic length and time scales of MD and the macroscopic length and time scales (microns to mm and μs to s) of finite element analysis (FEA). Only by establishing this connection from microscale to macroscale it is possible to build first principles methods for describing the properties of new materials and systems. Our aim is to reach the domain of materials science and engineering by building from fundamental principles of physics and chemistry. Thus, for fundamental predictions to play a direct role in materials innovation and design, it is mandatory to bridge the micro-macro gap.

In this scenario, we try to fill this gap in the case of controlled delivery of proteins from silicon membrane nanochannels. In particular, we use molecular simulations to calculate molecular parameters to be subsequently included in an appropriate mathematical equation of diffusion. In so doing, the proposed ansatz constitutes an "*ab initio*" recipe, for which no experimental data are needed to predict the protein release, and can be tailored in principle to match any different protein and any different surface.

Now, proteins accumulate at interfaces, a property that can be both a problem and a practical asset. Indeed, the adsorption of proteins at solid/liquid interfaces has enabled the development of diverse biomedical applications, such as biosensors, immunological tests, and drug-delivery schemes. Thus, the desire to control, understand, predict, and manipulate protein adsorption has been, and currently is, the main driving force for active research in this field. The strength of interaction between a particular protein and an impenetrable surface depends on the protein three-dimensional structure, and on the chemical nature of the surface. The complex, and substantially non-reversible, nature of protein adsorption at solid surfaces suggests that there is not one single driving force determining the free energy of the adsorption process. Hence, it is difficult, if not somewhat dangerous, to attempt generalizations about factors influencing specific examples of protein interfacial behavior. However, a thermodynamic inventory of the various interactions that contribute to protein adsorption can be summarized as follows (Claesson et al., 1995; Horbett and Brash, 1995; Norde and Zoungrana, 1998; Dickinson, 1999; Nakanishi et al., 2001). The origins of these interactions can be found in intermolecular forces, such as van der Waals forces, Coulombic attractions/repulsions, Lewis acid-base forces, and more entropically-based effects such as hydrophobic interactions, conformational entropy variations, and restricted mobilities. In addition, the adsorption process depends on intramolecular forces within the protein that might lead to an alteration of protein conformation. As a result, one sometimes finds a large difference between protein adsorption and desorption behavior, leading to an apparent irreversibility of the adsorption process. Generally speaking, proteins tend to adsorb more extensively and less reversibly at hydrophobic surfaces than at hydrophilic surfaces. With increasing degree of hydrophobicity of the surface, the ease of exchange of adsorbed protein molecules with the bulk aqueous phase is generally reduced. This difference can be attributed to a greater degree of unfolding at hydrophobic surfaces following protein adsorption, which leads to the development of strong interfacial hydrophobic interactions and associated displacement of vicinal water molecules from the unfavorable environment of the surface. In contrast, electrostatic protein-surface interactions tend to be more important at hydrophilic surfaces, especially for 'hard' proteins (which exhibit little conformational flexibility in the native state, and are held together strongly by intramolecular physical and covalent bonds), which may undergo very small changes in conformational structure upon adsorption.

The extent of globular protein unfolding upon adsorption is dependent on the protein structure. Little or no structural change following adsorption is expected for a 'hard' protein, such as lysozyme; accordingly, the effective thickness of the globular protein monolayer is often close to the known size of the native protein molecule in solution. Depending on surface coverage and molecular shape, however, some differences

may be expected in the interfacial orientation. When the shape of a given protein may be roughly inscribed in a rectangular prism with molecular dimensions of $a \times b \times c$, it is usually considered that there are two types of configurations for the adsorbed layer, i.e., one with a long axis (*end-on*) and one with a short axis (*side-on*) perpendicular to the surface. Sometimes, the type of configuration is estimated simply from the amount of protein adsorbed. However, the thickness, as well as the amount of the adsorbed layer, is required in order to obtain more detailed information. Further evidence for rather minimal change from the native structure with certain proteins comes from the retention of enzymatic activity on the adsorbed state. 'Soft' proteins show greater loss of ordered secondary structure (especially α-helices) on adsorption than do 'hard' proteins. Even for the same 'soft' protein, however, the extent of structural change may vary considerably depending on surface coverage, temperature, pH, and so on.

The degree of crowding in the adsorbed layer has also considerable influence on the degree of conformational change. The lower the adsorbed amount, the more space the protein has to spread out at the surface, and hence the greater the opportunity for unfolding to minimize the configurational free energy following adsorption. Early adsorbing proteins tend to exhibit a large loss of enzymatic activity, and are poorly exchangeable with the bulk phase after adsorption. Late adsorbing proteins tend to retain more enzymatic activity due to less unfolding and more participation in loosely held multilayers. The maximum adsorbed amount is determined by the rate of unfolding at the surface in relation to the rate of adsorption. Fast adsorption gives less time for protein molecules to spread out at the surface; consequently, the area occupied per molecule is lower and the adsorbed amount higher.

Experimental studies have done much in untangling the intricate role played by each of the components described above and in determining the large-scale interactions, structure, and surface rheology of adsorbed protein layers at interfaces. Nevertheless, the complexities encountered in these phenomena are such that in many cases different and somewhat quite contrasting explanations of the observed experimental results can be advanced. Mathematical modeling and computer simulations of such systems, apart from providing a certain unique insight of their own, allow a critical examination of such experimentally inferred explanation to be undertaken. In particular, molecular simulation methods such as Monte Carlo (MC) and molecular dynamics (MD) techniques have very recently opened avenues in the theoretical study of protein/surface interactions, because physical forces (as opposed to chemical bonding) are mainly expected to occur (Latour, 1999; Zhdanov and Kasemo, 2001; Castells et al., 2002; Raffaini and Ganazzoli, 2004; Liu and Haynes, 2004; Agashe et al., 2005). The MC set of computational techniques offers the non-negligible advantage of providing an efficient sampling of the conformational phase space, although for practical reason it is often restricted to coarse-grained models, which ineluctably neglect the true stereochemical features of proteins, and therefore yield only general results. In particular, all local details, including the secondary structure, are ignored. Additionally, the computational efficiency of MC methods rely on the assumption of a lattice model which, in principle, may set severe constraints if not affect the results. On the other hand, MD simulations follow the time evolution of a given molecular system and can be carried out at constant temperature. Moreover, atomistic-level models in continuous space are typically employed in MD simulations, thus yielding in principle realistic predictions about both the kinetics and the thermodynamics of the simulated process. As a drawback, MD methods are much more computationally intensive, and often a reliable sampling of the conformational phase space may be sometimes difficult to achieve. Accordingly, conformational changes taking place at very long times might be missed.

In this framework, the main objective of the present paper is to investigate the interaction of a well-known protein—hen egg-white lysozyme (HEWL)—with a pure silicon surface. This, as anticipated above, with the ultimate goal of evaluating molecular energetic and structural parameters which will be subsequently used in a macro-scale dynamical model of diffusion of HEWL through silicon-based nanochannels membranes developed in the companion paper (Amato et al., 2006). In this way, we show that it is possible *to predict* the kinetics of biomolecular diffusion through membrane nanochannels without recurring, in principle, to expensive laboratory experiments. The characterization of the diffusion dynamical properties of such membranes plays an important role in the medical setting since they are used in a number of clinical applications (Amato et al., 2006).

We carried out the simulations according to the following ansatz: (a) direct energy minimizations of the protein close to the silicon surface, and (b) MD runs with explicit solvation over 10 ns. The first procedure should correspond, in principle, to the initial adsorption stage, but it should also yield the preferred conformations if the adsorption process is either under kinetic control, or at large surface coverage. Conversely, the second procedure should yield the best overall conformation on a clean surface with the largest interaction energy under thermodynamic control.

2 Computational details

All simulations were carried out with the AMBER 7 suite of programs (Case et al., 2002). Starting from the available X-ray structures of the hen egg-white lysozyme (HEWL) (Protein Data Bank (PDB) entry codes 1 HEL) (Wilson et al.,

1992), we added all hydrogen atoms to the protein backbone and side chains with the *parse* module of AMBER 7. All ionizable residues were considered in the standard ionization state at neutral pH. To achieve electroneutrality, a suitable number of counterions were added, in the positions of largest electrostatic potential, as determined by the module *cion* within AMBER 7. The geometry of added hydrogen was refined for 200 steps (steepest descent) *in vacuum*. The all-atom force field (FF) parameter sets (*parm94*) by Cornell et al. was applied (Cornell et al., 1995), using the *sander* module of AMBER 7. The entire protein was then fully optimized up to an energy gradient lower than 10^{-3} kJ/molÅ.

The silicon surface was prepared from scratch. We first built a single plane of silicon using appropriate templates from the simulation package *Materials Studio* (v. 3.2, Accelrys Inc., San Diego, CA, USA), and saturated with hydrogen atoms the dangling bonds at the edges. After full optimization *in vacuum*, we replicated this plane to obtain a final surface of 84 Å × 65 Å.

A unit cell with periodic boundary conditions in three dimensions was then constructed, containing the silicon slab, the protein, and free mobile explicit water molecules of the TIP3P type (Jorgensen et al., 1983), and with the following cell size given as $X \times Y \times Z$, where the X and Z axes are parallel to the surface plane and Y is normal to the surface plane: 84 Å × 90 Å × 65 Å. After the placement of the protein, the remainder of the unit cell was filled with random water molecules. Any water molecules that overlapped with the protein, the fixed water slab, or the silicon surface were discarded, and additional random waters were added, until the average water density was 1 gcm^{-3}. Once constructed, the solvated assembly was subjected to energy minimization for 1000 steps using the steepest descent integrator, followed by 10 ps of MD simulations at 300 K and 1 atm pressure, using the constant NPT algorithm of Berendsen et al. (1984), with a coupling constant of 0.2 ps. Integration of the dynamical equations was carried out with the Verlet algorithm (Verlet, 1967), and the application of the *shake* algorithm (Ryckaert et al., 1977) to constrain all bonds to their equilibrium values, thus removing high frequency vibrations. Following this 'relaxation' phase, the productive MD simulations were performed in the canonical (NVT) ensemble, again at $T = 300$ K. A cutoff value $r_{\mathrm{vdW}} = 1$ nm was set for the calculation of van der Waals nonbonded interactions, whilst $r_{\mathrm{Coul}} = 1.8$ nm was selected for the electrostatic interactions. During all MD simulations, the atoms in the silicon surface were fixed (held invariant). The main justification for fixing the positions of the surface was that the frequencies of the vibrations in the silicon slab were high relative to the vibration in polypeptides and water, and running the simulations at time steps sufficiently small to resolve surface movement (and ensure computational stability) would have rendered the computation exceedingly long, if feasible. To determine the effect of fixing the silicon atom positions upon the measured quantities, we run preliminary simulations in which the terminal silicon atoms and their respective hydrogens were allowed to move. As expected, there was no significant difference between simulation with mobile and nonmobile groups.

Two 10 ns simulations were run: one with the protein and the surface, and one system that served as a control, with HEWL alone in water. The MD trajectories were analyzed for structural changes in the protein looking at the root-mean-square deviation (RMDS) of the protein structure compared to the energy-minimized crystal structure, and the change in the solvent-accessible surface area (SAS) of the protein (Lee and Richards, 1971). This was accomplished using the *surfinder* program developed in house. This software calculates the total accessible and molecular surface areas, and their polar, nonpolar, and charged components. The translational and rotational motions of the protein over the silicon surface were also analyzed by two routes: (1) tracking the vertical surface separation distance (VSSD) between the center of mass (COM) of the protein and that of the surface, (2) following the rotational motions of the protein over the surface, and (3) quantifying the eventual spreading process of the protein onto the surface.

In order to reduce computational time to reasonable limits, for the calculation of the protein/protein interaction energy we represented bulk solvent as a continuum, using a new method of scaling the charges (Schwarzl et al., 2003). In this case, the simulation cell consisted of a lysozyme molecule adsorbed onto the silicon surface, and a free lysozyme molecule. For the sake of simplicity, the bound HEWL molecule was modeled adsorbed onto the silicon surface in the most stable position, and we considered that the free HEWL molecule would sit on top of the bound one upon adsorption. Each simulation, carried out by keeping the silicon surface atoms static, was repeated six times, starting from six different rotational orientations of the free polypeptide. These orientations were the same considered for the study of the adsorption of HEWL on the silicon surface. The distance of the free HEWL from the bound HEWL was then changed, and the simulation repeated until 19 different protein distances were evaluated. The resulting interaction energies were then averaged, and the corresponding standard deviations were recorded.

All simulations were run on a Silicon Graphics Octane (both single and dual processor R12 K) cluster computer system, with a calculation time of about 2 days per nanosecond of simulation for the selected protein-surface system. The Chimera software (Pettersen et al., 2004) was used for visualization of the MD trajectories and for preparing all molecular illustrations.

3 Results and discussion

Lysozyme from hen egg-white (HEWL) is a small ($3 \times 3 \times 4.5\,nm^3$) $\alpha + \beta$ protein with a large a-domain containing four helices, and a 3_{10}-helix, and a smaller β-domain consisting of a triple-stranded anti-parallel β-sheet, an irregular loop containing two of the total four disulphide bridges and a 3_{10}-helix (see Fig. 1(a)).

Some details on the secondary structure and of the amino acids comprised within the principal structural motifs of HEWL considered are reported in Table 1, together with the respective hydropathy indexes calculated through the Kyte-Doolittle scale by summing the values of the constituent amino acids (Kyte and Doolittle, 1982). We recall that a positive hydropathy value indicates hydrophobicity, and a negative one hydrophilicity. Table 1 shows that HEWL comprises secondary motifs of different hydropathy indices, although amino acids of unlike character are present in all cases, irrespective of the overall index. Indeed, as shown also in Fig. 1(b), not all hydrophobic residues (colored gold) are hidden in the protein interior. The estimated apolar content of the interior of HEWL is about 60%, which is typical of most small globular proteins. Moreover, polar and apolar residues are more or less evenly distributed over the protein surface (see Fig. 1(b)); no regions are observed where the surface shows either a distinctly hydrophilic or hydrophobic character.

Table 1 Amino acids and secondary structure of hen egg white lysozyme, with hydropathy indices

Motif	First amino acid	Last amino acid	No. of amino acids	Hydropathy index
α-helix I	Arg5	Arg14	10	−2.8
α-helix II	Leu25	Ser36	12	+3.9
α-helix III	Thr89	Ser100	12	+5.4
β-strand I	Thr43	Arg45	3	−8.7
β-strand II	Thr51	Tyr53	3	−5.5

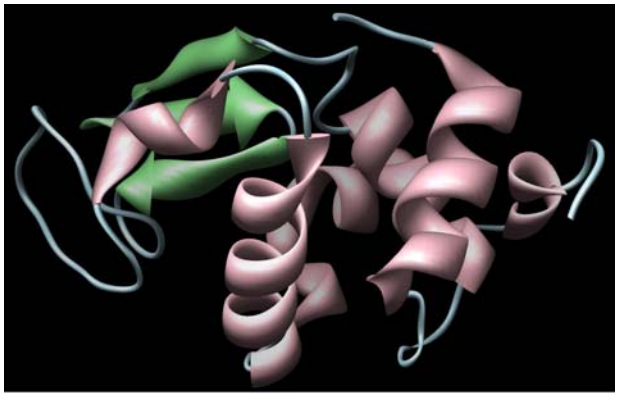

(a)

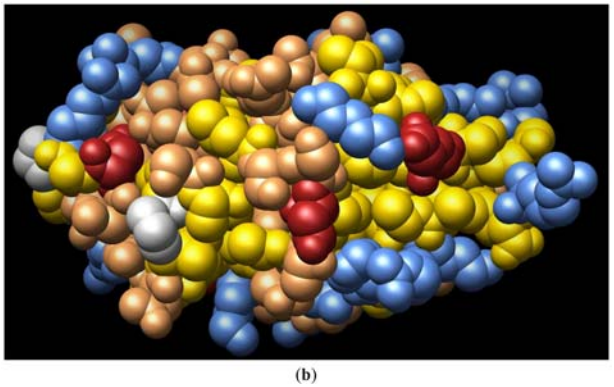

(b)

Fig. 1 (a) Ribbon representation of the hen egg-white lysozyme showing the protein main structural motifs: α-helices (pink), β-sheets (green) and loop/coils (light blue). (b) CPK representation of the distribution of residues at the protein surface. Color scheme: non-polar residues, gold; positively charged residues, blue; negatively charged residues, red; polar residues, light brown

According to our procedure, we firstly optimized the geometry of the isolated HEWL protein. The minimized energy, to be used later to calculate the interaction energy with the silicon surface, amounted to 4.62 MJ mol^{-1}. As expected, we observed relatively small differences between the optimized and the experimental geometries of the two structures. Afterward, we optimized the geometry of the protein close to the silicon surface, keeping the latter fixed. Due to the homogeneous distribution of residues on the protein surface, we considered six different starting HEWL orientations, as shown in Fig. 2. Upon direct energy minimizations, all six orientations showed a significant initial surface adsorption, usually accompanied by very confined rearrangements of the interacting motifs.

The results of the initial optimizations are summarized in Table 2. The lowest energy minimum, corresponding to the most stable state found by this procedure (position 3 in Table 2 and in Fig. 2), amounts to 1.26 MJ mol^{-1}, and the energies for the other minima are reported relative to this value. The corresponding geometry is reported in Fig. 3(a), while part b of the same Figure shows the geometry of the highest energy minimum (position 6 of Table 2 and Fig. 2).

Table 2 Results of initial energy minimizations

Position	E_{rel} [a]	E_{int} [b]	E_{strain} [c]	$n_{5\,Å}$ [d]
1	0.74	2.33	0.39	40
2	0.25	3.43	0.49	57
3	0	3.77	0.44	57
4	0.88	2.79	0.38	36
5	1.34	1.64	0.23	26
6	1.80	1.01	0.19	17

[a] E_{rel} = total energy relative to the lowest-energy state found in the initial minimization; [b] E_{int} = interaction energy of the protein with the surface; [c] E_{strain} = molecular strain energy; [d] $n_{5\,Å}$ = number of amino acids at a distance less than 5 Å from the plane. All energies are in MJmol^{-1}.

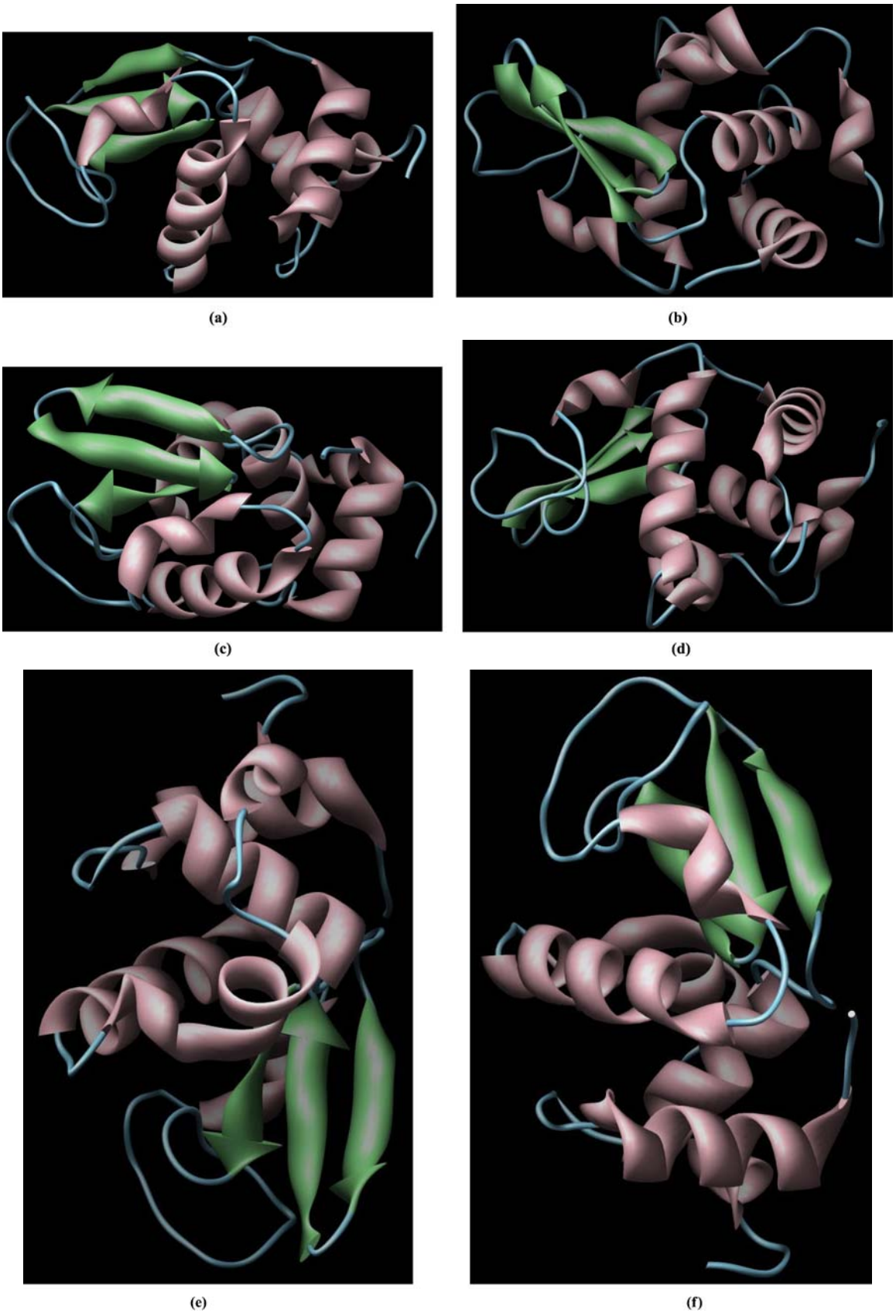

Fig. 2 Cartoon of the hen egg-white lysozyme oriented according to the six directions considered for close approach to the silicon surface. (a), position 1; (b) position 2; (c) position 3; (d), position 4; (e), position 5; (f), position 6

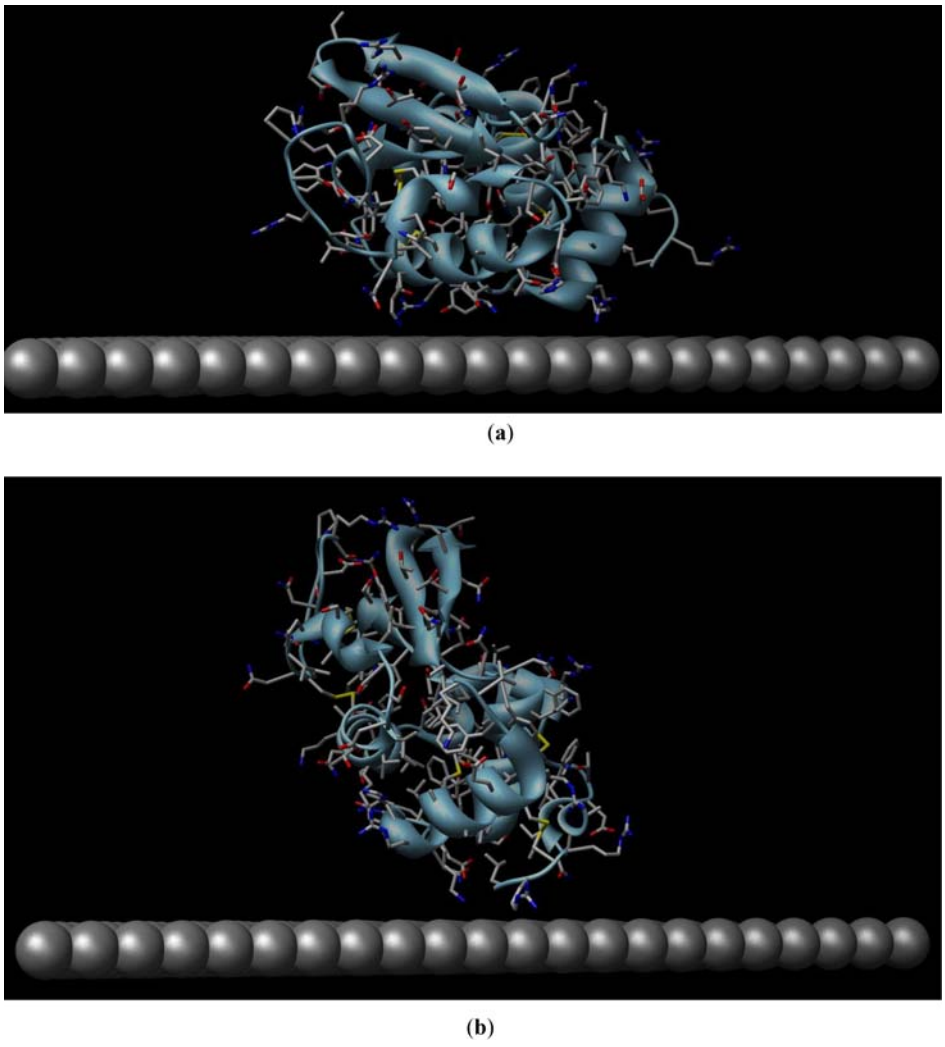

Fig. 3 Illustration of the lowest energy minimum configuration (a), and of the highest energy minimum configuration (b) of HEWL over the silicon surface. Water molecules and hydrogen atoms have been omitted for clarity

Very little intramolecular rearrangements can be detected in the optimized geometry of the most stable initial adsorption state shown (as well as upon adsorption in the less stable state), so that the geometry of the lysozyme molecule and its secondary structure are essentially unchanged.

In addition to the relative energy of the initial adsorbed state (E_{rel}), Table 2 reports also the interaction energy, defined as $E_{\text{int}} = (E_{\text{free}} + E_{\text{plane}}) - E_{\text{tot}}$, where E_{free} is the energy of the free, isolated molecule in the optimized geometry. According to this definition, $E_{\text{int}} > 0$ is the energy required to desorb the protein from the surface and bring it back to the free state. Also, since the silicon plane was kept fixed in the simulations, we have $E_{\text{plane}} = 0$, although of course all the silicon atoms do correctly interact with the protein atoms. We also define $E_{\text{strain}} = E_{\text{frozen}} - E_{\text{free}}$, where E_{frozen} is the energy of the lysozyme in the frozen geometry it adopts upon adsorption.

Let us now describe the rearrangements found through these initial energy minimizations. In all cases, the motifs close to the surface locally optimize the interaction, but this process does not substantially perturb the secondary structure, as shown in Fig. 3. The driving force consists of the favorable van der Waals interactions with the hydrophobic surface, mainly due to the hydrophobic or at least the less hydrophilic residues. Thus, E_{int} can be as large as 3.77 MJ mol^{-1} for the most stable orientation, to be compared with the value of 1.01 MJ mol^{-1} for the less stable adsorbed state. Considering that the lysozyme model used is composed by 129 residues, these values correspond to 29 and 8 kJ mol^{-1} per amino acid. It is also interesting to point out that the E_{strain}, which originates from the surface-induced local rearrangements, roughly follows the same trend as E_{int}, amounting, for instance, to 0.44 and 0.19 MJmol^{-1} for the above-mentioned geometries. However, stronger interactions with the surface largely compensate for the greater strain energy mainly due to broken H-bonds of the regular motifs. Stronger interactions are related with a larger number of residues in contact with the surface, irrespective of their hydropathy index, thanks to the apparently random distribution of hydrophobic and hydrophilic residues. Thus, we find

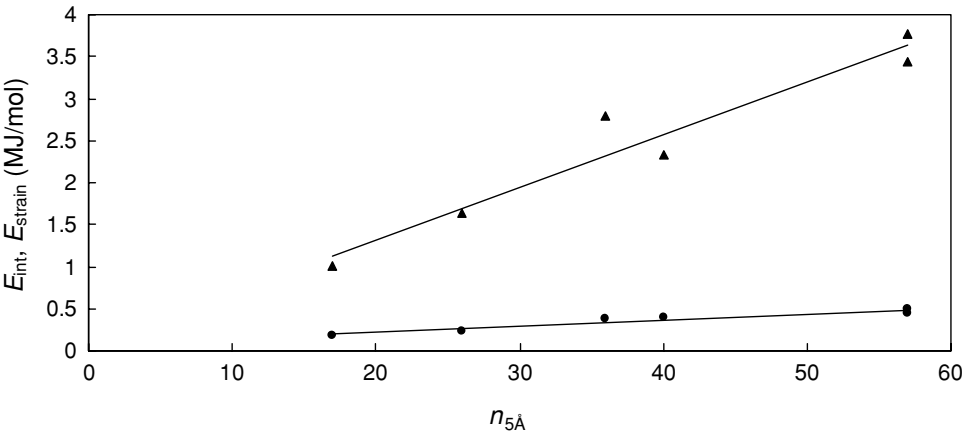

Fig. 4 Interaction energy E_{int} (triangles) and strain energy E_{strain} (circles) of lysozyme over the silicon surface after the initial energy minimizations in various orientations plotted as a function of $n_{5\,Å}$, the number of amino acids being in contact with the surface at a distance less than 5 Å. Lines represent the best-fit lines through the origin given by Eqs. (1) and (2). The corresponding correlation coefficients are $R^2 = 0.936$ and 0.843

a significant positive correlation between both E_{int} and E_{strain} and the number of amino acids in contact with the surface, $n_{5\,Å}$, also reported in Table 2 (we conventionally take 5 Å as the upper limit for the contact distance with the surface). Such correlation is shown in Fig. 4, where E_{int} and E_{strain} are plotted as a function of $n_{5\,Å}$. The best-fit lines through the origin for the lysozyme protein are given by:

$$E_{int} = 63 n_{5\,Å}\,\mathrm{kJ\,mol^{-1}} \quad (1)$$

$$E_{strain} = 9 n_{5\,Å}\,\mathrm{kJ\,mol^{-1}} \quad (2)$$

In other words, in the initial adsorption stage only minor readjustments are found in the HEWL structure, by virtue of its globular pattern, leading however to a small interaction energy for initial adsorption even in the most favorable orientation. As already stressed, the residues hydropathy is qualitatively less important because of the presence of unlike amino acids in all secondary motifs, and of the cooperative nature of the adsorption process. From Eqs. (1) and (2) we see that E_{int} increases with the number of residues in contact with the surface faster than E_{strain}. This feature implies that the lysozyme molecule could optimize its surface interaction with larger deformations than those reported in Fig. 3. Accordingly, the geometries obtained through these initial minimizations correspond to local energy minima achieved in the initial adsorption stage. Thus, the thermodynamically most stable adsorption state is eventually reached only once some free-energy barrier is overcome. The energy input required to overcome this barrier could be attained through MD simulations by the kinetic energy, as described below.

The lowest energy geometry found by direct energy minimization in the previous section was subjected to MD runs to explore the eventual change in conformation. Following the recent and elegant approach of Latour (Agashe et al., 2005) the extent of the structural change undergone by HEWL was firstly monitored by the-root mean-square deviation (RMSD) from the minimized structure. In particular, RMSDs were monitored during the entire MD simulation to quantify the change in protein structure over time, or the opening of protein folds to expose previously buried residues. The RMSD results for HEWL on the silicon surface and in bulk water are shown in Fig. 5(a) and (b), respectively.

As expected, the first instant of the simulation reveal the most marked change in RMSD, which reflects the mobility of the amino acids on the protein surface. After approximately 3.5 ns, the value of RMSD stabilizes around the average values of 2.5 Å and 2.8 Å for the protein in bulk solvent and over the surface, respectively. Looking globally at the protein structure, this does not exhibit substantial changes during the MD simulation. Interestingly, HEWL over the silicon surface exhibits almost the same behavior of the control system in plain water, reflecting similar effects. In quantification of the visual inspections, the behavior of RMSDs in Fig. 5(a) and (b) show that only relatively small further changes in protein structure take place by virtue of specific interactions between the silicon surface atoms and the functional groups present on the protein surface. Finally, it seems probable that the HEWL protein has reached a quite stable configuration on the silicon surface, given the long time simulated and the stable trend of the RMSD.

Figure 6(a) and (b) illustrates the evaluated change in solvent accessible surface (SAS) for the control and the HEWL/surface system, respectively. Here, the polar, nonpolar, and total SAS of the protein are computed as they were represented alone in the bulk water. Thus, a decrease in the SAS value would not indicate contacts between HEWL and surface, with subsequent exclusion of water, but rather a compaction of the biomacromolecular structure with a consequent reduction in its surface area. Contrarily, an increment in the SAS value should represent the unfolding of the protein to expose previously buried amino acids. As we can see from Fig. 6(a) and (b), no meaningful variation can be envisaged in the total SAS, as well as in its components, both for the control protein and for the system including the silicon

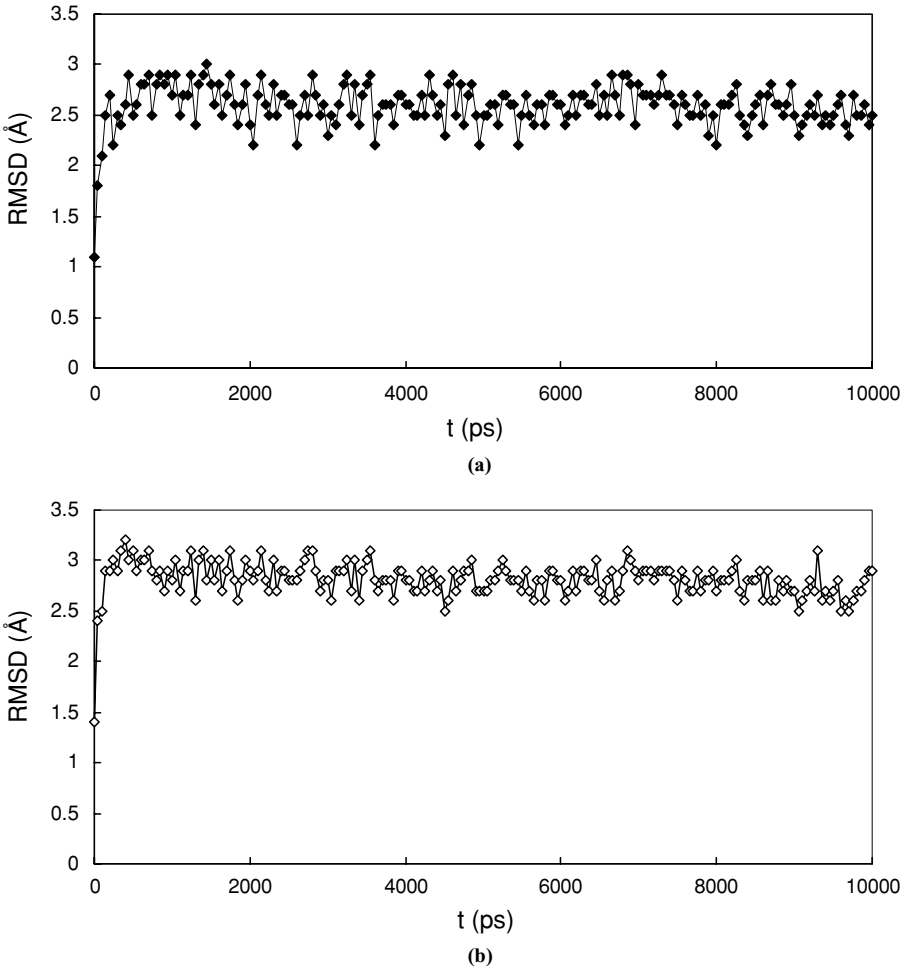

Fig. 5 (a) Root-mean-square deviation (RMSD) values of HEWL in bulk water, and (b) over the silicon surface

surface. This can be taken as an indication that the silicon surface does not induce any substantial protein unfolding over the surface itself during the course of the MD simulation. Furthermore, the curves in Fig. 6(a) and (b) suggest that the changes in RMSDs reflect only relative motion about a stable core protein, as expected for 'hard' proteins such as HEWL, as opposed to any significant changes in the global protein conformation.

Importantly, from the MD simulation of the HEWL alone in water we also calculated the molecular volume of the protein, $V_{\mathrm{vdW,HEWL}}$, by averaging the value of the van der Waals volume of different saved snapshots over the equilibrated trajectory. The resultant value is $V_{\mathrm{vdw,HEWL}} = 16651$ Å^3.

From the stored atom positions of HEWL, taken from the MD trajectory, we can also calculate a number of other, relevant quantities in order to visualize the adsorption and eventual motion/spreading of the protein onto the surface. The position of the protein is reflected in the position of its center of mass (COM), which is defined as:

$$\mathbf{R}_{\mathrm{COM}} \equiv \frac{\sum_{i=1}^{N} m_i \mathbf{r}_i}{\sum_{i}^{N} m_i} \tag{3}$$

where m_i is the mass of the i-th atom, and N is the number of atom in the protein. This $\mathbf{R}_{\mathrm{COM}}$ can subsequently be used to calculate a vertical distance of the HEWL molecule to the surface (VSSD):

$$Y_{\mathrm{COM}} = \mathbf{R}_{\mathrm{COM}} \cdot \mathbf{e}_Y \tag{4}$$

where $\mathbf{e}_Y$ is the unit vector in the Y-direction (i.e., vertical) of the Cartesian coordinate system. The eventual spreading process can be monitored by following the evolution of the parallel radius of gyration of HEWL, defined as:

$$R_{g\|}^2 \equiv \frac{\sum_{i=1}^{N} m_i((\mathbf{r}_i - \mathbf{R}_{\mathrm{COM}})^2 - ((\mathbf{r}_i - \mathbf{R}_{\mathrm{COM}}) \cdot \mathbf{e}_{\mathrm{Y}})^2)}{\sum_{i=1}^{N} m_i} \tag{5}$$

The approach of HEWL to the silicon surface during the MD simulation is nicely monitored by the time dependence of the VSSD Y_{COM}, as defined by Eq. (4), and reported relative to the protein initial position in Fig. 7(a). In this way, positive values of Y_{COM} indicate that the center of mass of HEWL translated further away for the silicon surface, compared with its initial position, whilst negative values

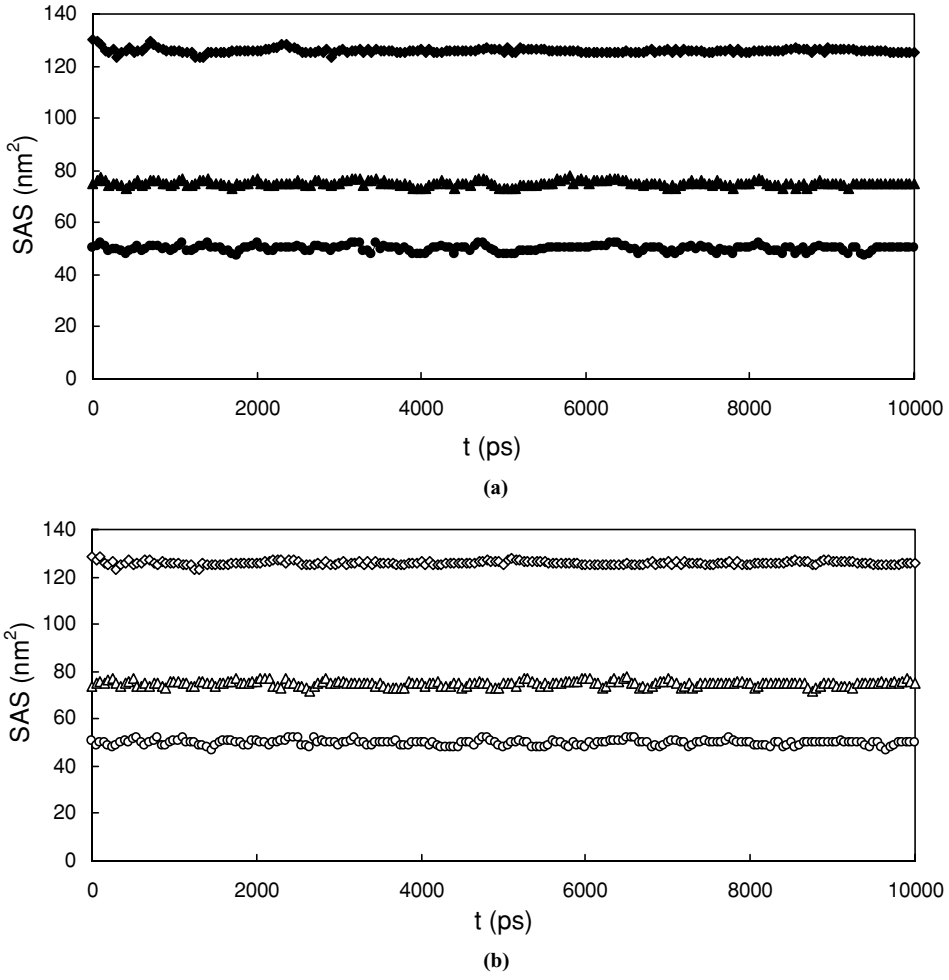

Fig. 6 (a) Change in total (top data line), nonpolar (middle data line), and polar (bottom data line) SAS of HEWL in bulk water, and (b) over the silicon surface

of this quantity indicate translations closer to the surface plane. From this plot we can observe how, after some initial drifting away from the silicon surface, the HEWL molecule feels the surface attraction and moves closer to the surface where, after 4.5 ns, it seems to attain a relatively constant distance, approximately 1 nm closer with respect to its initial position.

The eventual spreading of the protein onto the surface can be checked by considering the time behavior of $R^2_{g\|}$ reported in Fig. 7(b). The fact that the parallel size of the HEWL radius of gyration only slightly increases from its initial value of 1.96 nm^2 to the average, constant value of 2.14 nm^2 is a notable indication that no spreading of the protein is clearly visible over the surface, as could be expected for the 'hard' protein HEWL, whose tertiary conformation is also stabilized by the presence of 4 sulfide bridges. These evidences, coupled with the information gathered from the analysis of the RMSD, indicate that HEWL does not unfold on the hydrophobic, silicon surface during the 10 ns of MD simulations.

The planar motion of the protein over the silicon surface can be also estimated starting from the coordinated (x, y, and z) of the center of mass of HEWL as extracted from the relevant MD trajectory. The net displacement of the protein on the silicon plane can be calculated as:

$$r_p = \sqrt{(dX^2 + dZ^2)} \tag{6}$$

in which $dX = X(t) - X(0)$ and $dZ = Z(t) - Z(0)$, t being time, and $X(0)$, $Y(0)$, and $Z(0)$ representing the protein initial position, where the X and Z orthogonal axes are parallel to the surface plane, and Y is normal to the surface plane. As defined, r_p yields an indication of the translational motion of the protein parallel to the surface. Figure 7(c) illustrates the planar motion of HEWL on the surface, with its center of mass translating over the surface, primarily due to the rolling motion of the protein over the surface itself.

The visual inspection of the MD trajectory file reveals that, during the simulation period, the HEWL molecule undergoes a rotation motion over the silicon surface, in search of a local minimum energy position, while establishing a series of hydrophobic interactions between the surface silicon atoms and the side chains of the protein surface residues. Two different

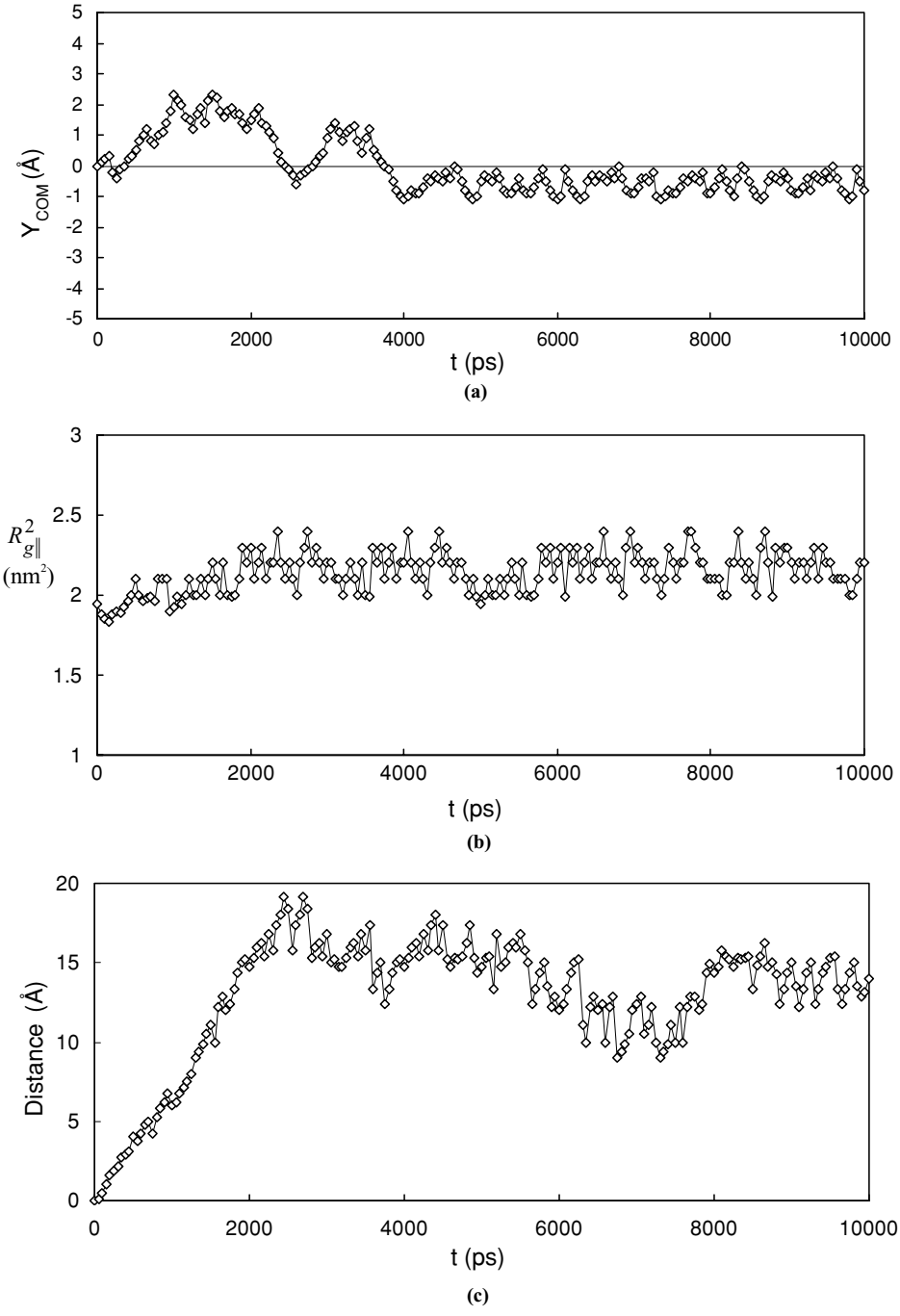

Fig. 7 (a) Vertical distance (Y_{COM}) of the HEWL center of mass to the silicon surface surface. (b) Time behavior of $R^2_{g\|}$ for HEWL over the silicon surface. (c) Motion of HEWL parallel to the planar surface

snapshots, which clearly illustrate the protein rotations, are reported in Fig. 8(a) and (b). In its motion, the protein rolls over the surface until it is able to orient itself by exposing several hydrophobic residues facing the surface. This position is then stabilized by favorable interactions through the side chains of nonpolar residues such as alanine, leucine, isoleucine, and valine, lying close to the surface. The trajectory revealed in details that only the apolar protein residues did interact strongly with the surface, whilst the polar and ionic residues remained hydrated and well separated from the surface.

From all the foregoing discussion we can conclude that the long MD simulation conducted on HEWL over a silicon surface predicts that the protein molecule is able to reorient itself on the hydrophobic surface over time, by exerting favorable hydrophobic interactions via its nonpolar residues. As partially expected for 'hard' proteins, HEWL does not show any remarkable level of structural change during the entire simulation course. On the other hand, the protein showed a manifest tendency to rotate and translate upon the surface, in order to achieve a preferred orientation, allowing for maximizing the attractive, stabilizing hydrophobic forces.

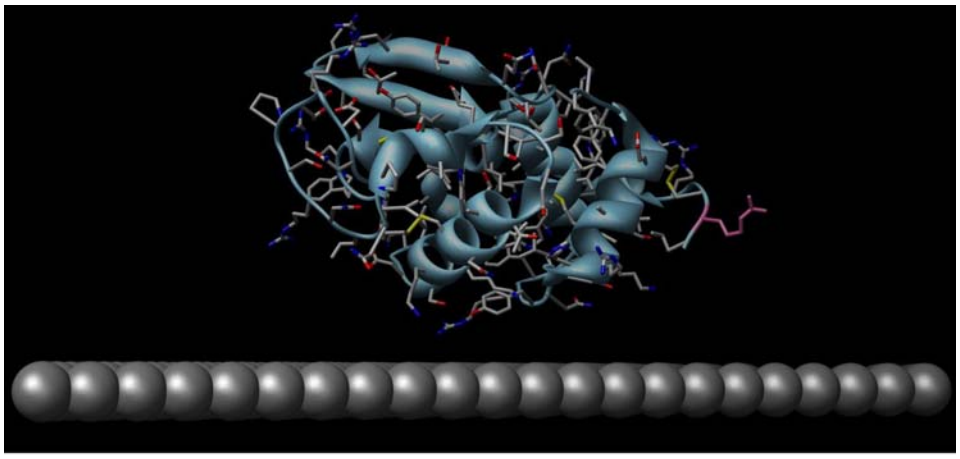

(a)

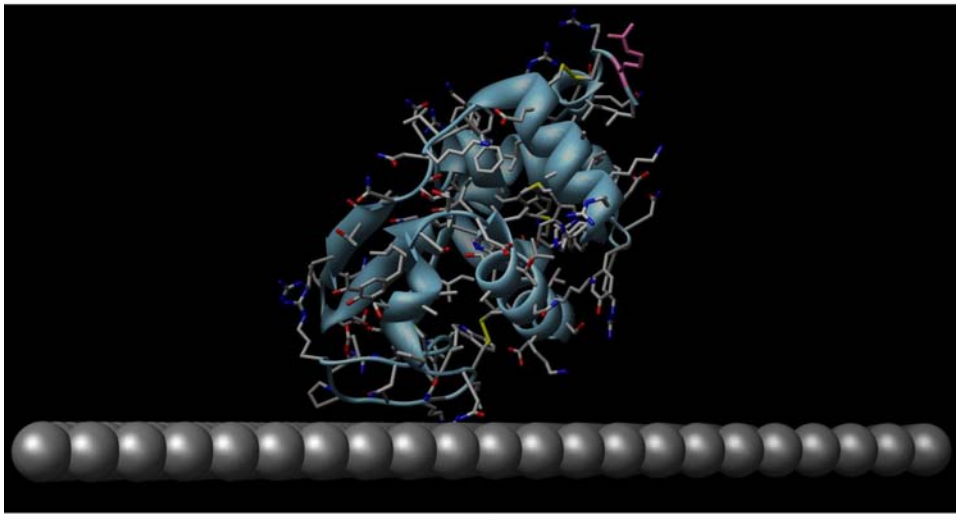

(b)

Fig. 8 Snaphsots from the 10 ns MD simulation trajectory, showing HEWL rolling over the silicon surface. (a) position after 1 ns. (b) position after 2 ns. The extent of the rotation can be qualitatively appreciated by considering the change in position of residue Arg128, colored pink in both images. Water molecules and hydrogen atoms have been omitted for clarity

Keeping in mind the ultimate goal to obtain, from molecular simulations, an entire set of parameters necessary to predict the diffusion of protein in nanochannels, we finally determine the energy of attraction between a lysozyme chain adsorbed onto the silicon surface and another, free lysozyme molecule. For the sake of simplicity, we considered that the free HEWL molecule would sit on top of the bound one upon adsorption. Each simulation, again carried out by keeping the silicon surface atoms static, was repeated six times (i.e., starting from the same six different rotational orientations of the free polypeptide illustrated in Fig. 2). The distance of the free HEWL from the bound HEWL was then changed, and the simulation repeated until 19 different protein/protein distances were evaluated. The resulting interaction energies were then averaged, and the corresponding standard deviations were recorded. Figure 9 shows a plot of the interaction energies on the free HEWL as a function of position from the HEWL adsorbed onto the surface. As we can see, the interaction energy follows the standard particle dispersion interaction pattern: a very repulsive potential at close distances, followed by an attractive region, and ending with forces approaching zero at long distances. In details, the energy becomes negligible at distances greater than 5–6 Å, is at a minimum at approximately 2.5 Å, and become increasingly repulsive as the free polypeptide approaches the bound protein. The average calculated value at the minimum is equal to $E_{\min} = -93.93$ kJ/mol.

All the above-discussed evidences from simulation are in sound agreement with the available experimental information, according to which lysozyme can form a 60 Å bilayer at pH = 7, corresponding to a bilayer of sideways-on adsorbed proteins (Lu et al., 1998). At the same time, the high value of the interaction energy between HEWL and the silicon surface calculated in this work is in harmony with the evidences yielded by Haynes and Norde, according to which adsorption of HEWL on a hydrophobic surface is irreversible with respect to dilution (Haynes and Norde, 1995). Similarly, no HEWL desorption occur with increasing or decreasing pH over a range 2–12, or with increasing temperature up to 95°C. Further, the fact that, at high surface coverage adsorbed

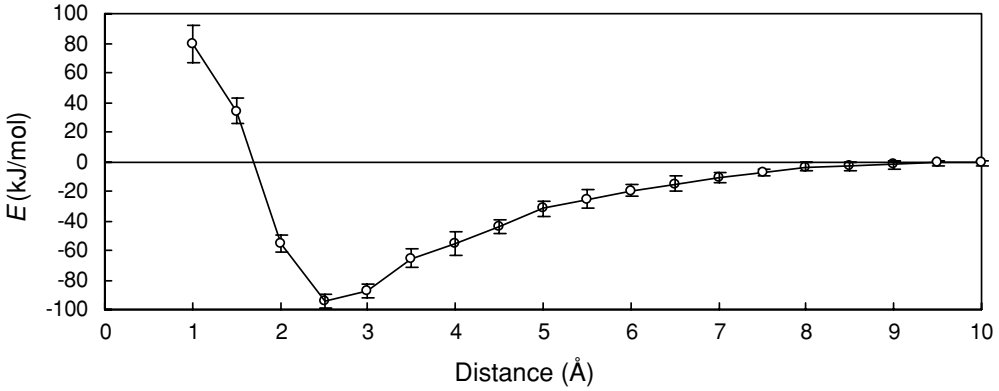

Fig. 9 Free/bound HEWL interaction energy as a function of position from the HEWL molecule bound to the silicon surface. Each data point is given as an average of the six different values corresponding to the six different orientations of the free HEWL with respect to the bound HEWL

HEWL conformations on the surface do not depend strongly on the protein bulk concentration and, thus, on the concentration gradient driving diffusion of the protein to the surface, lead to the conclusion that steady-state conformations of the adsorbed HEWL appear to depend on the balance between the intermolecular forces, which stabilize the native-structure of HEWL, and the strong intermolecular forces between the adsorbed protein and the sorbent surface, as well evidenced by our simulations. All these evidences concur to the conclusion that the conformational dynamics of the adsorbed molecules are rather limited once the system has reached the steady-state.

4 Conclusions

One of the reasons we undertook this study was to understand the way in which a protein such HEWL adsorbs to a synthetic surfaces, and how this process of adsorption can be used to quantify its influence the diffusion process of this biomacromolecule in a silicon nanochannel membrane. The global behavior that emerges from the simulation suggests that the kinetics of HEWL orientational changes on the silicon surface can be much faster than those of adsorption-induced conformational changes. If true, then the thermodynamic "landscape" of adsorption energy as a function of protein orientation can have a deep implication for drug-delivery system (DDS) design. Indeed, under these conditions, adsorbed proteins have the tendency to translate and rotate over the surface toward the nearest local energy well, following their initial adsorption onto the surface, with the nature of the surface chemistry sensibly determining the final distribution of adsorbed protein orientations on the surface. Conformational changes can then take place, but only after this reorientation stage of the adsorption process has occurred. If a material surface for a DDS could be designed so as to present to the adsorbing protein an energy landscape with ideally only one thermodynamically significant minimum energy orientation, the orientation of adsorbed proteins could theoretically be controlled. Tuning surface chemistry in this manner to guide protein adsorption into desired orientations could thus potentially turn in favor, providing much better control over protein adsorption process and, hence, of the ultimate diffusion and release process. Control over conformational changes of the protein could likewise then be achieved as a second stage in the overall adsorption process.

If, on the other hand, the kinetics of conformational changes were much faster than the kinetics of reorientation, then proteins would tend to spread out over the surface in whatever orientation they happened to be when they were first adsorbed, without time to reorient, and surface tailoring could have little effect on the orientation of adsorbed macromolecules. The former hypothesis, which is supported by our results, provides a much more desirable situation in terms of the potential to control the behavior of adsorbed proteins and their subsequent diffusive activity, by the rational design of surface-tailored DDS.

This work was indeed performed with the main objective of investigating the behavior of HEWL on silicon surface via molecular simulations, in order to obtain some information at the molecular level useful for implementation on mathematical modeling of diffusion of proteins in silicon nanochannel membranes. The overall variations in RMSD and SAS for HEWL on a pure silicon surface over the long 10 ns MD simulation period were found however not to differ much from those of a control system consisting of the same protein in bulk water. This can be taken as an indication of the fact that the adsorption process does not induce any substantial level of conformational change in the protein conformation, at least over this time span. At the same time, the molecular simulation evidences imply that, following the initial adsorption, HEWL undergoes substantial surface-induced rotational and translational motions, until relatively stable low-energy adsorbed orientations are achieved. It must be

emphasized here, however, that the described adsorption behavior of HEWL can be expected to be substantially influenced by the presence of other protein molecules in the environment. As the computational power continues to increase, and simulation techniques at higher (meso) scales become at the same time available, ensemble of HEWL should be able to be simulated, and these effects should be able to be addressed directly. Despite the current limitations, the observation that the kinetics that control changes in adsorbed protein orientation may be much faster than the kinetics that control adsorbed protein conformation is of great relevance, as it suggests that a proper tailoring of the surface of a DDS may be exploited to control the orientation of adsorbed proteins independently of adsorbed conformation, thus influencing the ultimate macroscopic property of the DDS.

While much development work is still needed, molecular simulations have enormous potential to complement experimental studies, as we strive to understand the complexities of protein-surface interactions, and how to control/exploit them, so that the inherent properties of proteins can be effectively harnessed for uncountable applications in nano-bio-medical applications.

Acknowledgments MCC, RW and MF are grateful to the National Cancer Institute and BRTT of the State of Ohio for their support of this work. This project has been partially funded by National Cancer Institute, National Institute of Health under Contract No. NO1-CO-12400. SP, MF and MF acknowledge the generous financial support from the Italian Association for Cancer Research (AIRC), grant 2955.

References

M. Agashe, V. Raut, S.J. Stuart, and R.A. Latour, Langmuir **21**, 1103 (2005).

F. Amato, C. Cosentino, S. Pricl, M. Ferrone, M. Fermeglia, and M. Ferrari, Biomed. Microdev. this issue (2006).

H.J.C. Berendsen, J.P.M. Postma, W.F. van Gunsteren, A. DiNola, A., and J.R. Haak, J.R. J. Chem. Phys. **81**, 3684 (1984).

D.A. Case, D.A. Pearlman, J.D. Caldwell, T.E. Cheatham III, J. Wang, W.S. Ross, C.L. Simmerling, T.A. Darden, K.M. Merz, R.V. Stanton, A.L. Cheng, J.J. Vincent, M. Crowley, V. Tsui, H. Gohlke, R.J. Radmer, Y. Duan, J. Pitera, I. Massova, G.L. Seibel, U.C. Singh, P.K. Weiner, and P.A. Kollman, AMBER 7 (University of California, San Francisco, CA, 2002).

V. Castells, S. Yang, and P.R. Van Tassel, Phys. Rev. E **65**, 31912 (2002).

P.M. Claesson, E. Blomberg, J.C. Fröberg, T. Nylander, and T. Arnebrant, Adv. Coll. Interf. Sci. **57**, 161 (1995).

W.D. Cornell, P. Cieplak, C.I. Bayly, I.R. Gould, K.M. Merz, D.M. Ferguson, D.C. Spellmeyer, T. Fox, J.W. Caldwell, and P.A. Kollman, Am. Chem. Soc. **117**, 5179 (1995).

E. Dickinson, Coll. Surf. B**15**, 161 (1999).

C.A. Haynes and W. Norde, J. Coll. Interf. Sci. **169**, 313 (1995).

T.A. Horbett and J.L. Brash (Eds.) Proteins at Interfaces II: Fundamentals and Applications (American Chemical Society, Washington, DC, 1995).

W.L. Jorgensen, J. Chandrasekhar, J.D. Madura, R.W. Impey, and M.L. Klein, J. Chem. Phys. **79**, 926 (1983).

J. Kyte and R.F. Doolittle, J. Mol. Biol. **157**, 105 (1982).

R.A. Latour, Curr. Op. Solid State Mat. Sci. **4**, 413 (1999).

B. Lee and F.M. Richards, J. Mol. Biol. **55**, 379 (1971).

S.M. Liu and C.A. Haynes, J. Coll. Interf. Sci. **275**, 458 (2004).

J.R. Lu, T.J. Su, P.N Thirtle, R.K. Thomas, A.R. Rennie, and R. Cubitt, J. Coll. Interf. Sci. **206**, 212 (1998).

K. Nakanishi, T. Sakiyama, and K. Imamura, J. Biosci. Bioeng. **91**, 233 (2001).

W. Norde and T. Zoungrana, Biotechnol. Appl. Biochem. **28**, 133 (1998).

E.F. Pettersen, T.D. Goddard, C.C. Huang, G.S. Couch, D.M. Greenblatt, E.C. Meng, and T.E. Ferrin, J. Comput. Chem. **25**, 1605 (2004).

G. Raffaini and F. Ganazzoli, Langmuir **20**, 3371 (2004).

J.P. Ryckaert, G. Ciccotti, and H.J.C. Berendsen, Comput. Phys. **23**, 327 (1977).

S.M. Schwarzl, D. Huang, J.C. Smith, and S. Fisher, In Silico Biol. **3**, 187 (2003).

L. Verlet, Phys. Rev. **159**, 98 (1967).

K.P. Wilson, B.A. Malcolm, and B.V. Matthews, J. Biol. Chem. **267**, 10842 (1992).

V.P. Zhdanov and B. Kasemo, Proteins: Struct., Funct., Genet. **42**, 481 (2001).